Characterization of the 5-HT$_7$ Receptor. Determination of the Pharmacophore for 5-HT$_7$ Receptor Agonism and CoMFA-Based Modeling of the Agonist Binding Site

Erik S. Vermeulen,*,† Anne W. Schmidt,‡ Jeffrey S. Sprouse,‡ Håkan V. Wikström,† and Cor J. Grol†

Department of Medicinal Chemistry, Center for Pharmacy, State University of Groningen, A. Deusinglaan 1, NL-9713 AV Groningen, The Netherlands, and Department of Neuroscience, Pfizer Global R&D, MS 8220-4178, Groton, Connecticut 06340

Received February 27, 2003

On the basis of a set of 20 diverse 5-HT$_7$ receptor agonists, the pharmacophore for 5-HT$_7$ receptor agonism was determined. Additionally two CoMFA models were developed, based on different alignments of the agonists. Both models show good correlations between experimental and predictive pK_i values and show a high degree of similarity. The CoMFA fields were subsequently used to map the agonist binding site of the model of the 5-HT$_7$ receptor. Important roles in ligand binding are attributed to Asp162 of TM3 (interaction with a protonated nitrogen), and Thr244 of TM5 (interaction with a substituent at an aromatic moiety). Amino acid residues of the aromatic cluster of TM6 are hypothesized to play an important role in ligand binding as $\pi-\pi$ stacking moieties. Agonists missing a hydrogen-bond-accepting moiety, but possessing an aromatic substituent instead, seem to bind the receptor with high affinity as well by occupying a lipophilic pocket hosted by residues of TM5 and TM6.

Introduction

The most recently discovered member of the serotonin receptor family, the 5-HT$_7$ receptor, has received great interest over the past decade.[1−5] Four splice variants have been identified, with main differences at the C-termini, suggesting different efficiencies in G-protein coupling. However, all isoforms seem to be positively coupled to adenylyl cyclase.[6−8] Despite the fact that several series of antagonists with moderate to high affinity and selectivity for the 5-HT$_7$ receptor have been synthesized in the recent years,[9−12] its (patho-) physiological role still remains unclear. It has been hypothesized to be involved in the regulation of circadian rhythms,[13−17] depression,[18,19] and smooth muscle relaxation,[20,21] but this awaits further elucidation with the use of known and newly synthesized selective ligands (both agonists and antagonists) and relevant in vivo models.

In general, development of rationally designed new compounds for targets lacking 3-D structural information demands well-defined pharmacophore models. Therefore, it is essential to have a comprehensive series of functionally identical ligands at one's disposal. Recently, the first pharmacophoric hypotheses for 5-HT$_7$ antagonism were presented. Based on either a set of 30 antagonists[12] or a mix of 5-HT$_7$ agonists and antagonists,[22] these models offer a valuable contribution to the development of novel 5-HT$_7$ ligands. Nevertheless, it should be emphasized that the validity of the model of Lopez-Rodriguez et al. is limited to ligands with antagonistic properties only. The use of both agonists and antagonists by Wilcox et al. resulted in a validated CoMFA model for 5-HT$_7$ receptor affinities. However, the model does not discriminate between agonistic and antagonistic properties. Furthermore, these models offer no revelation of receptor−ligand interactions, which additionally forms an important tool in understanding the mechanism of action at the binding site of the receptor and the design of new compounds.

We wish to report the development of the first pharmacophore model for 5-HT$_7$ receptor agonists and a 3-dimensional CoMFA model, based on a set of 20 5-HT$_7$ receptor agonists. In addition, we developed a receptor model based on the α-carbon template for the helical parts of the structure of rhodopsin-like receptors.[23] The binding site of the receptor model was characterized by means of the contour maps of the 3-D CoMFA model and the mutual interaction points of the set of ligands to locate and orientate the side chains of the hypothesized ligand binding amino acid residues.

Ligands Used for Development of the CoMFA Model. Pharmacological data, as listed in Table 1, of compounds **1**−**4**, **12**, **15**−**20** were taken from the literature.[4,5,24−27] Compounds **5**−**11**, **13**, and **14** were synthesized in our laboratories according to the synthesis routes depicted in Scheme 1 (**5**−**7**), Scheme 2 (**8**−**11**, **13**), and Scheme 3 (**14**) and were fully characterized using IR, ^{1}H NMR, ^{13}C NMR, and GCMS and were chemically pure according to these techniques and TLC. All compounds have been reported previously. Pharmacological data of the synthesized compounds were determined at Pfizer laboratories.

3-D QSAR of 5-HT$_7$ Receptor Agonists. Full conformational analysis of the set of 20 5-HT$_7$ receptor agonists in their protonated form (Figure 1) was performed in MacroModel,[28] except for **20** (neutral), and followed by a pharmacophore-identifying procedure through ligand overlap using APOLLO.[29] Thus, the

* Corresponding author. Tel: +31 50 311 8007. Fax: +31 50 363 6908. E-mail: e.s.vermeulen@farm.rug.nl.
† State University of Groningen.
‡ Pfizer Global R & D.

10.1021/jm030826m CCC: $25.00
Published on Web 11/05/2003

Table 1. Ligand Geometries, Experimental Pharmacological Data, and Predicted p*K*i Values from CoMFA Computations

ligand	distance (Å) centroid−H-bond acceptor	distance (Å) centroid−N^+	H-bond acceptor−N^+	expl pK_i	n	% increase basal AC	predicted A1	predicted A2
1	2.755	6.017	6.954	9.22 ± 0.01[e]		nd[e]	9.59	9.44
2	2.767	5.997	6.881	9.03 ± 0.05[e]		nd[e]	8.80	8.91
3	3.648	6.014	6.533	9.92 ± 0.04[e]		100	9.91	10.07
4	2.766	6.032	6.931	8.10 ± 0.01[e]		nd[e]	7.83	7.84
5	2.766	6.007	6.888	6.20 ± 0.01	4	39	6.46	6.28
6	2.766	6.029	6.924	5.95 ± 0.02	3	17	6.10	6.04
7	2.766	6.032	6.931	7.40 ± 0.05	3	92	7.12	7.28
8	2.775	5.241	7.918	5.80 ± 0.07	3	58	5.88	5.92
9	2.755	5.273	5.228	6.91 ± 0.01	3	73	6.89	6.96
10	2.755	5.273	5.228	7.06 ± 0.03	3	73	6.96	7.08
11	2.755	5.273	5.228	7.47 ± 0.07	3	92	7.23	7.35
12	2.755	5.273	5.228	7.34 ± 0.05[e]		nd[e]	7.50	7.34
13	2.796	5.297	5.257	6.47 ± 0.05	3	99	6.52	6.54
14	2.773	6.446	7.072	7.69 ± 0.01	3	25	7.61	7.55
15	nd	6.446	nd	7.74 ± 0.02[e]		nd[e]	7.85	7.77
16	2.770	5.581	5.059	6.90 ± 0.03[e]		nd[e]	6.96	6.96
17	5.905	5.182	4.520	8.02 ± 0.04[e]		nd[e]	7.88	7.94
18	4.038[a]	5.260	7.547[b]	9.08[e]		nd[e]	9.10	9.07
19	4.274[a]	5.260	7.722[b]	9.60[e]		nd[e]	9.60	9.59
20	4.281[a]	5.008[c]	7.888[d]	7.79 ± 0.08[e]		nd[e]	7.94	7.78

[a] Distance centroid−centroid of substituent. [b] Distance centroid of substituent−N^+. [c] Distance centroid−4,5-dihydroimidazole N(H). [d] Distance centroid of substituent−4,5-dihydroimidazole N(H). [e] Agonist activity reported in the literature.[4,5,24−27]

Scheme 1. Synthesis of Tryptamines[a]

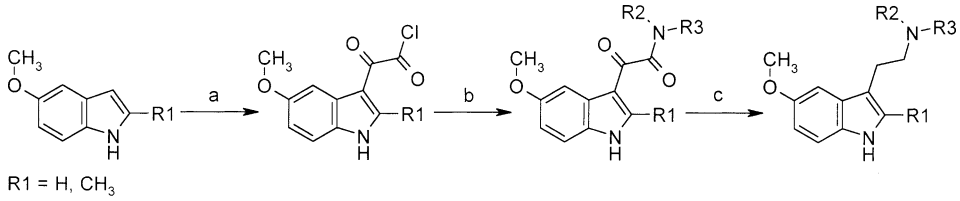

[a] Reagents and conditions: (a) oxalyl chloride, ether. (b) amine, $H_2O/CHCl_3$. (c) $LiAlH_4$.

Scheme 2. Synthesis of 2-Aminotetralines[a]

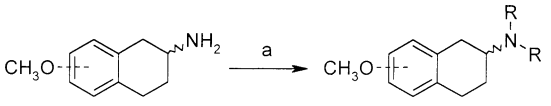

[a] Reagents and conditions: (a) aldehyde, $NaCNBH_3$, EtOH, AcOH, rt.

positively charged nitrogen of the ligands was defined as a hydrogen-bond-donating moiety and the oxygen atom of the substituent at the six-membered aromatic ring (if present) as hydrogen-bond-accepting. In LSD (**17**), the carbonyl oxygen of the ethyl−amide moiety was defined as a hydrogen-bond-accepting group. Additionally, a centroid was defined perpendicular to the plane of the six-membered aromatic ring. The centroid of **14** and **15** was defined for the six-membered ring not substituted with the piperazine moiety, and in **19** the aromatic ring of the aminotetraline moiety was used for this purpose. In case of **20**,[24] which lacks a protonated, positively charged amino group, the NH of the 4,5-dihydroimidazole ring served as the hydrogen-bond-donating moiety, and the centroid of the methyl-bearing phenyl ring was used for overlap with aromatic rings of the other ligands.

In the first alignment [Figure 2 upper panel, alignment 1 (A1)], APOLLO (RMSFit module) calculated, energy dependently, the best overall least-squares fit of the extension vectors (defined by APOLLO's Vecadd module) of the hydrogen-bond-forming functional groups and defined centroids of all conformations of each ligand in the set. This provided us with a set of 20 superimposed ligands, surrounded by the 3-dimensional orientation of mutual interaction points belonging to the putative receptor binding site, as calculated by APOLLO.

A second alignment was considered as well, since it appeared that aromatic substituents as in compounds **18**−**20** could function as an alternative for the absence of a hydrogen-bond-accepting moiety, nevertheless resulting in the agonistic behavior of the ligands. In this second alignment procedure [Figure 2, bottom panel, alignment 2 (A2)], all ligands were superimposed by fitting only the extension vectors of the H-bond-donating nitrogen substituent and the centroid of the aromatic ring of all conformations of each compound. With the exception of **8**, we expected major differences in alignment for tryptamines only, since the aminotetralines were already superimposed very accurately onto the structure of **16**, due to more similarities between the rigid bicyclic moieties with respect to the ergoline structure.

The two sets of superimposed ligands (A1 and A2) were subsequently used for computation of the two closely related 3-D CoMFA models in Sybyl.[30] From the spatial orientation of A1, the distance between the two hydrogen-bond-donating and -accepting receptor dummies (i.e. the mutual interaction points) was measured and equaled 8.0 Å. Other geometric parameters, describing the minimum pharmacophoric parameters for 5-HT_7 receptor agonist binding of the set of 20 ligands, are listed in Table 1 and schematically depicted in Figure 3. The mutual interaction points of all ligands that were calculated by APOLLO are mimicked by

Scheme 3. Synthesis of 7-Methoxynaphthylpiperazine[a]

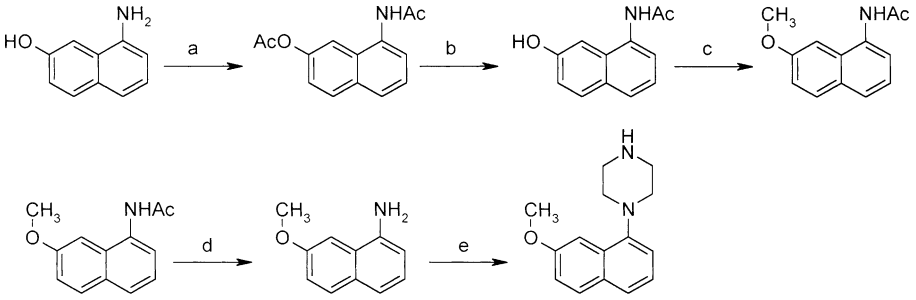

[a] Reagents and conditions: (a) TEA, Ac_2O, $CHCl_3$. (b) $NaHCO_3$ (sat.), CH_3OH. (c) dimethyl sulfate, NaOH (1 N), acetone. (d) HCl, EtOH. (e) bis(2-chloroethyl)amine, chlorobenzene, reflux

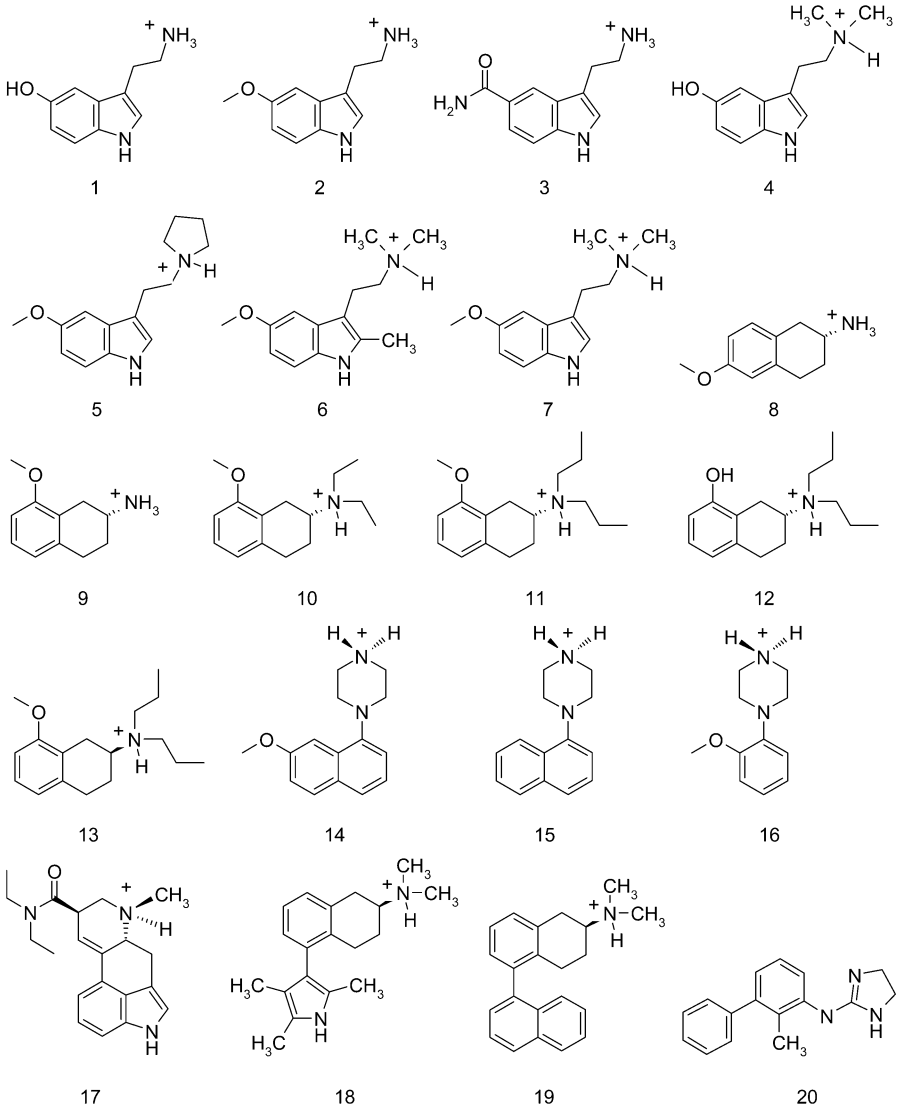

Figure 1. Chemical structures of ligands **1**−**20**.

means of water molecules. The relative orientation of these interaction points of A1 (i.e. putative receptor binding site dummies) was subsequently used in our receptor model to locate and orientate the side chains of the amino acid residues that presumably play an important role in ligand binding.

3-D Orientation of Mutual Interaction Points of Known Ligands. The two sets of superimposed ligands A1 and A2, surrounded by the 3-dimensional orientation of mutual interaction points belonging to the hypothesized receptor binding site, as calculated by APOLLO, are depicted in Figure 2. According to A1, all tryptamines are oriented similarly with minor deviations, due to slightly different alignments based upon the H-bond-accepting moieties (upper left panel). For the aminotetralines (upper middle panel), both rings of the 8-substituted derivatives are almost perfectly superimposed onto the structure of **17**, whereas for the 5-substituted derivatives, the rings are oriented equiplanar with the 8-substituted aminotetralines, though rotated slightly around the centroid of the aromatic ring. The orientation of **8** is significantly different in order to form

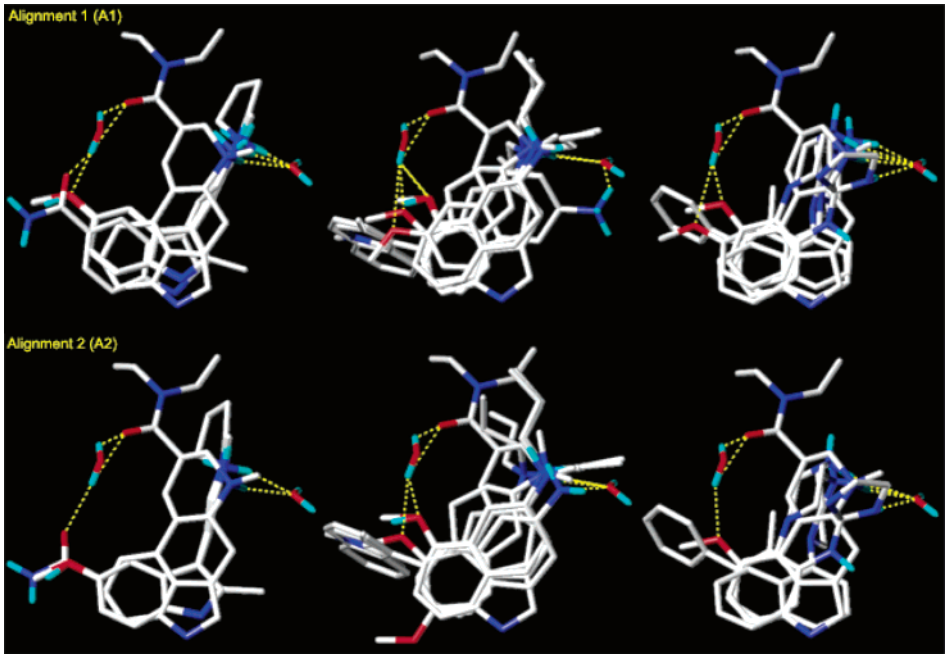

Figure 2. Three-dimensional orientation of superimposed ligands with mutual interaction points. LSD with tryptamines (A1, upper left), **17** with aminotetralines (A1, upper middle), **17** with the remainder of the ligands (A1, upper right), **17** with tryptamines (A2, bottom left), **17** with aminotetralines (A2, bottom middle), **17** with the remainder of the ligands (A2, bottom right). Dotted yellow lines are hydrogen bonds between mutual interaction points and ligands.

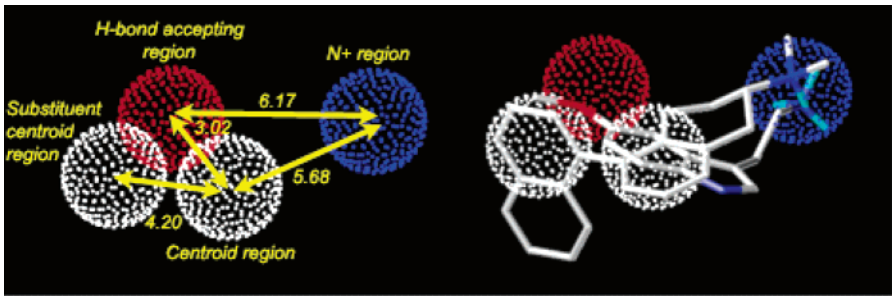

Figure 3. Hypothesized pharmacophoric features of 5-HT$_7$ receptor agonists. Average dimensions are in angstroms (left). Ligand **1** and **19** superimposed onto pharmacophore (right).

hydrogen bonds with the mutual interaction points with both the methoxy and the amino substituents. The superimposed ligands **14**−**16** and **20** are oriented predominantly equiplanar with their aromatic rings with respect to the six-membered aromatic ring of **17**, while the hydrogen-bond-donating nitrogen atoms are oriented in the direct vicinity of the positively charged nitrogen atom of **17**. The orientation of the hydrogen-bond-donating NH group of the 4,5-dihydroimidazole group of **20** is very well aligned with the structure of **17**, while the unsubstituted aromatic ring is oriented very similar to the 5-substituents of **18** and **19**. For A2, APOLLO selected the identical conformations of every ligand in the set for superimposing compared to A1. Confirming our predictions, the main differences in ligand alignment can be observed from the series of tryptamines (**1**−**7**; Figure 2, bottom left) and **8**: the indole nuclei and ethylamine side chains are perfectly superimposed, while now the orientation of **8** is similar to the orientation of the other 2-aminotetralines, with the methoxy substituent clearly oriented away from the mutual interaction point. As can be seen from the bottom panel of Figure 2, all the other ligands in A2 are similarly superimposed with respect to A1.

CoMFA Computations. On the basis of the set of 20 superimposed 5-HT$_7$ receptor agonists, we developed two CoMFA models, based on the two different alignments obtained by APOLLO. Sybyl standard parameters were used, with steric and dielectric cutoff values of 15 and 10 kcal/mol respectively (distance dependent dielectric function). For both alignments, six partial least squares (PLS) calculations were performed: five cross-validated (four groups) and one non-cross-validated. The results of these computations are summarized in Table 2. Only minor differences can be detected between both non-cross-validated PLS calculations (Table 1). The calculated R^2 values (0.978 vs 0.991) and standard errors of estimates (0.214 vs 0.138) are virtually identical for both alignments. The non-cross-validated PLS calculation of A1 showed a steric fraction of 0.759 and an electrostatic fraction of 0.241,and used 2373 (out of 2420) CoMFA columns. The corresponding values for A2 equaled 0.784 and 0.216 respectively, and in these computations 2119 columns were used (out of 2178). As a result of these closely corresponding results, the contour maps as shown by the molecular modeling software application were also very similar. Therefore,

Table 2. PLS Analysis of CoMFA Computations of A1 (upper set) and A2 (lower set)

run no.	R^2	optimum no. of components	mean SE of predictions	range of sep
		Alignment 1		
cross-validated (4 groups)				
1	0.965	1	0.364	0.229−0.468
2	0.973	1	0.341	0.203−0.482
3	0.951	1	0.440	0.273−0.609
4	0.970	1	0.319	0.212−0.439
5	0.973	1	0.316	0.203−0.411
non-cross-validated				
1	0.978	6	0.214	nd
		Alignment 2		
cross-validated (4 groups)				
1	0.685	6	0.959	0.798−1.242
2	0.643	6	0.999	0.850−1.263
3	0.715	6	0.946	0.747−1.313
4	0.627	6	0.954	0.861−1.154
5	0.660	5	1.011	0.812−1.273
non-cross-validated				
1	0.991	6	0.138	nd

the graphical reproduction of A2 is used for further analysis only, as depicted in Figure 5.

Homology Modeling of the Receptor. The sequence of 449 amino acids of the human 5-HT$_{7A}$ receptor was taken from the SwissProt database (entry P34969; http://us.expasy.org/sprot/). On the basis of the identification of evolutionary highly conserved amino acids within the rhodopsin-based family of G-protein coupled receptors, the helical parts of the receptor were manually aligned with a template of α-carbon atoms of the transmembrane domains.[23]

Initial minimization of the helices separately (Tripos force field, Gasteiger−Hückel charges, dielectric constant 5.0, distance dependent, conjugate gradient 0.1 kcal/mol/Å) and subsequent minimization of the ensemble of the seven transmembrane helices resulted in our model with a total energetic value lower than the sum of energies of the individually minimized helices. Careful examination of the hypothesized binding site of our model, located near the highly conserved Asp162 and enclosed by TM3, -5, -6 and -7, suggested that the mutual interaction points found by APOLLO, could represent the following amino acid residues: Asp162 of TM3 as the counterion for the protonated amino group, Thr244 of TM5 as the hydrogen-bond-donating residue toward the substituent of the aromatic ring, and Trp340 as the $\pi-\pi$ stacking moiety. Strikingly, no amino acid residue could be identified as suitable hydrogen-bond-accepting moiety for the indole NH. Cys339 in TM6 appears to be a possible candidate for this task, but is too far away from the other ligand binding residues in this model. Besides, from this set of ligands it cannot be concluded that this hydrogen-bond-donating moiety is part of the 5-HT$_7$ pharmacophore.

Mapping of CoMFA Model onto Receptor Binding Site. The CoMFA model with the highest R^2 value (A2, 0.991, standard error of estimate 0.138) was subsequently projected onto the binding site to identify conceivable amino acid residues that could account for the contour maps as computed during the comparative molecular field analysis. For this purpose, the 3-dimensional orientation of mutual interaction points, as

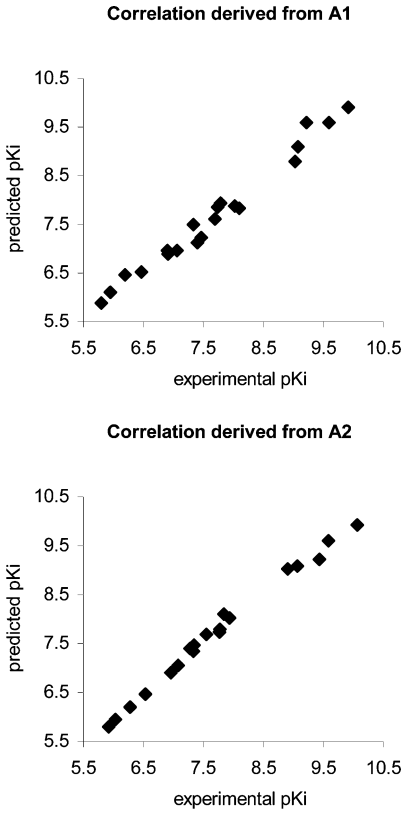

Figure 4. Graphical representation of correlation between experimentally observed pK_i values and predicted pK_i values for A1 and A2.

calculated from the preceding alignment procedure by APOLLO, were used to locate the ligand binding amino acid residues in the receptor binding site. Careful examination of this projection onto the imaginary inner sphere of the binding site basically indicated the most distinguishing amino acid residues (Figure 6). This way, the red contours (negative charge increases affinity) surrounding the hydrogen-bond-accepting moieties attached to the central aromatic ring of tryptamines and aminotetralines clearly indicated the hydrogen-bond-donating side chain of Thr244, and the blue contours (positive charge increases affinity) surrounding the positively charged nitrogen atoms indicated the negatively charged side chain of Asp162. The yellow areas (bulk decreases affinity) near the positively charged nitrogen atom of the ligands, forming the boundaries of the earlier mentioned lipophilic pocket, can be attributed to the side chains of TM3 (Ile159) and TM5 (Ile241) and TM7 (Phe369). The aromatic substituents of ligands 18−20 are surrounded by green molecular fields (bulk increases affinity). Notably, these green areas indicate a second lipophilic pocket formed by amino acids at the boundary surfaces of TM5 (Phe248) and TM6 (Phe336, Thr337, and Leu341).

Docking of Ligands in Binding Site. To complete this study, a number of the ligands (at least one of each class representing tryptamines, aminotetralines, ergoline, biphenylaminodihydroimidazole) were manually docked into the binding site as described and minimized to analyze the ligand binding interactions. As a starting point for minimization, the conformations of the ligands used for superpositioning in APOLLO were used, and the side chains of the hypothesized amino acid

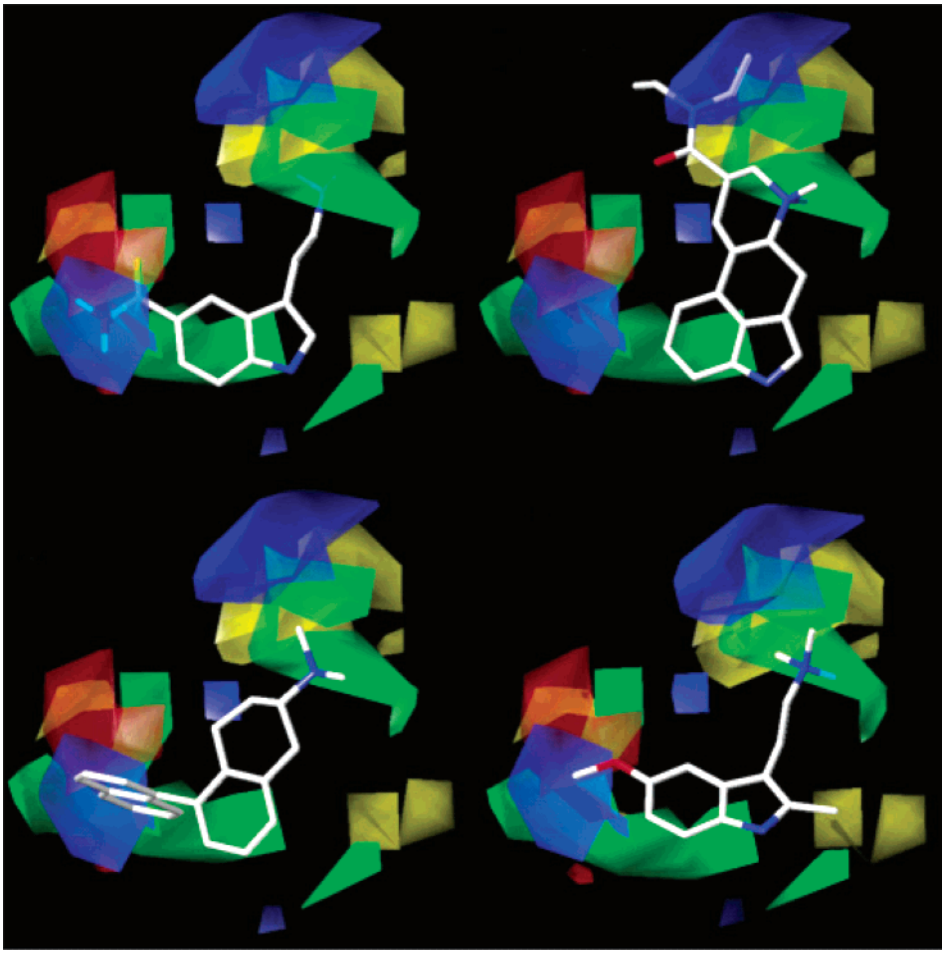

Figure 5. Graphical representation of CoMFA computations of A2 with example ligands **3** (upper left), **17** (upper right), **19** (lower left), **6** (lower right). Green indicates bulk favored, and yellow indicates bulk disfavored. Red indicates electronegative groups favored, and blue indicates electropositive groups favored. Contour map thresholds green/yellow 75/45; blue/red 85/15.

residues were adjusted, if necessary, to adopt the 3-dimensional orientation of mutual interaction points in the most optimal manor. Minimization (Tripos force field, Gasteiger-Hückel charges, NB cutoff 8.0, dielectric constant 5.0, distance dependent, conjugate gradient 0.1 kcal/mol/Å) resulted in properly docked ligands (Figure 7, **1** taken as an example). Hydrogen bonds are formed between Thr244 and the aromatic substituent (if present) at the six-membered aromatic ring of the ligands, and electrostatic interactions between Asp162 and the positively charged amino group present in all ligands (except **20**, where the dihydroimidazole NH moiety serves as H-bond donor). The aliphatic substituents attached to the positively charged nitrogen are hosted by a lipophilic cavity defined by amino acid residues of TM3 and TM5. Trp340 and Phe336, being part of the aromatic cluster of TM6 (Phe336-Trp340-Phe343) and therefore likely to play an important role in the activation of the receptor,[31] were able to form $\pi-\pi$ stacking interactions with the aromatic cores of all ligands. Notably, the aromatic side chains of Phe336, Trp340, and Phe343 of TM6 form a well-ordered stack of aromatic rings together with the central aromatic moiety present in all ligands of the set. The aromatic substituents of **18**, **19**, and **20**, were hosted in a lipophilic pocket surrounded by amino acid residues of TM5 and TM6. The binding energy was calculated as the difference of energies of the free ligand and the receptor model before complex formation and the energetic value of the receptor−ligand complex after minimization in Sybyl. All receptor−ligand complexes show lower energies than the sum of energies of free receptor and ligand.

Discussion

To identify a pharmacophore model for 5-HT_7 receptor agonists, a set of 20 agonists of wide chemical and structural diversity was investigated in their binding mode to the 5-HT_7 receptor. The choice for agonists was based on the assumption that agonists, being able to induce a conformational change of the receptor evoking an effect on the coupling of the G-protein, would have interactions with a specific binding place in the receptor in common. Antagonists (and inverse agonists), generally having more dissimilar chemical structures, might bind to more different places in the receptor transmembrane domain or the extra cellular site in order to block the evoking effect on G-protein coupling caused by agonists (or to foil the effect of constitutive activity).

On the basis of the set of ligands used in this study, it was initially hypothesized that one main feature of the pharmacophore model for 5-HT_7 receptor agonists (Figure 3) consists of a flat aromatic ring system with a protonated nitrogen capable of forming a directed, reinforced electrostatic interaction at a distance of 5.01−6.66 Å. Furthermore, the pharmacophore exhibits a hydrogen-bond-accepting moiety at a distance of 2.76−

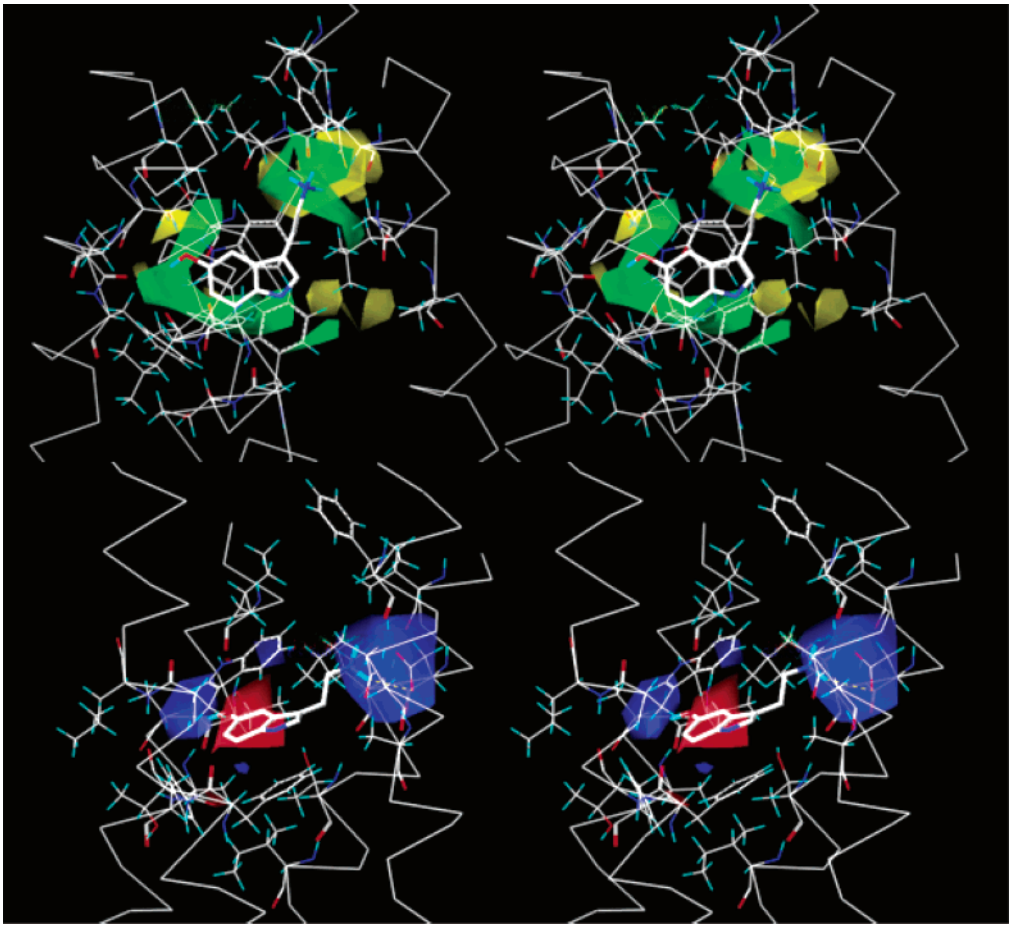

Figure 6. Two stereoviews of CoMFA projection onto binding site with **1** at the binding site in capped sticks. Green indicates bulk favored, and yellow indicates bulk disfavored. Red indicates electronegative groups favored, and blue indicates electropositive groups favored. Contour map thresholds green/yellow 75/45; blue/red 85/15.

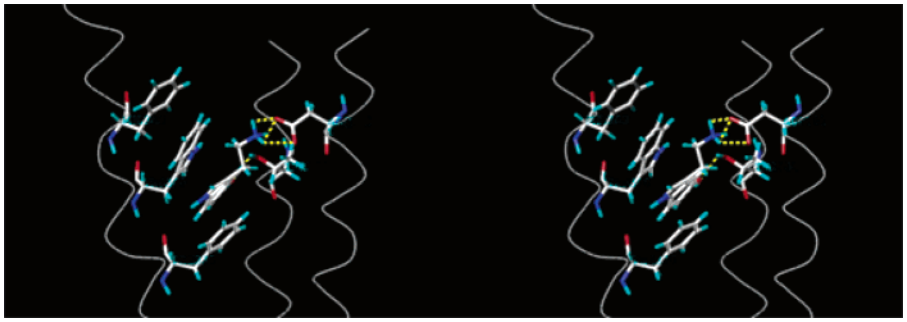

Figure 7. Stereoview of **1** docked into the binding site. Visible amino acid residues of TM3 (Asp162), TM5 (Thr244), and TM6 (Phe336, Trp340, and Phe343).

3.65 Å from the centroid of the central aromatic ring. Notably, the carbonyl oxygen atom of the carboxamide group of **17** is capable of forming a hydrogen bond with the same mutual interaction point from a distance of 5.91 Å, thereby compensating for the absence of such a moiety directly attached to the flat aromatic ring system. We suggest that the high binding affinity of 5-CT compared to the other tryptamines can be attributed to the double hydrogen-bond formation of the carboxamide group to the hydroxyl group of Thr244.

However, since **15** and the very recently presented ligands **18**, **19**, and **20** are short of a hydrogen-bond-accepting moiety, but nevertheless show moderate to high affinity for the 5-HT$_7$ receptor, the lack of this feature appears not to be insurmountable. Apparently, the deficiency of a hydrogen-bond-accepting moiety at the central aromatic ring system can be compensated by the presence of a flat aromatic ring system at a distance of 4.04−4.28 Å from, and almost perpendicular to, the central aromatic ring system, which can occupy a hypothesized lipophilic pocket hosted by residues of TM5 and TM6.

In our opinion, the residues of the aromatic cluster could play an important role in both receptor affinity and efficacy. From the docking studies performed (Figure 7), it appears that the central aromatic moieties present in all ligands of this series are properly stacked between the side chains of Trp340 and Phe343 of TM6 (part of the aromatic cluster) as a well-ordered pile of aromatic rings. It seems plausible that ligands lacking

this feature, or disrupting this well-ordered orientation due to steric interactions, negatively influence both binding affinity and efficacy. Previously performed docking studies of a number of ligands devoid of 5-HT_7 receptor affinity (data not shown) also confirm this hypothesis. Generally, these compounds disrupt the well-ordered pile of aromatic rings by either the characteristics of the ligand (aliphatic rings in skeleton cause steric repulsions) or the ligand has to adopt an orientation in order to bind to Asp162 and Thr244, causing similar disruption of the aromatic cluster.

Initially, it seemed puzzling that, within the series of tryptamines, larger substituents attached to the positively charged nitrogen atom reduce the affinity for the 5-HT_7 receptor, while the opposite appears to be true for the series of 8-substituted aminotetralines. However, this might be explained in terms of steric hindrance and lipophilicity. The average distance between the positively charged nitrogen atom and the central aromatic ring within the series of tryptamines and 8-substituted aminotetralines equals 6.02 and 5.27 Å, respectively. It is hypothesized that, within the series of aminotetralines, larger substituents can occupy a lipophilic pocket located near Asp162 of TM3 with increasing affinity for the receptor. Within the series of tryptamines, these larger substituents might contrarily experience increased steric interactions with the boundaries of this lipophilic pocket as a result of the more distant orientation of the nitrogen atom substituents with respect to the central aromatic ring system.

Strikingly, no amino acid residue could be identified as a suitable hydrogen-bond-accepting moiety for the indole NH. Cys339 in TM6 appears to be a possible candidate for this task, but it is too far away from the other ligand binding residues in this model. Besides, from this set of ligands it cannot be concluded that this hydrogen-bond-donating moiety is part of the 5-HT_7 pharmacophore. The affinities of the 2-aminotetralines and **14** and **15** underline this hypothesis.

The two different alignments A1 and A2 result in very similar CoMFA models. Only the alignment of **8** is shifted significantly, and the tryptamines are shifted marginally if the hydrogen-bond-accepting group is left out of consideration, while the different rules for alignment make no difference for the remainder ligands. Nevertheless, both alternatives were considered since agonists missing this feature show moderate to high affinity for the receptor as well. The R^2 values of model A1 and A2 (0.978 and 0.991, respectively), indicate both good correlation between experimentally derived and predicted pK_i values and a high degree of similarity between both models.

We acknowledge the fact that the biological data were obtained from assays using rat 5-HT_7 receptors, while our homology model is based on the human sequence of the 5-HT_7 receptor. However, we do not expect significant differences as a result of this discrepancy, since data have indicated a high degree of interspecies homology of the entire amino acid sequence and an even higher degree of homology if the TM domains are considered only.

We wish to emphasize the choice for the 3-D model developed by Baldwin[23] of α-carbon atoms of the transmembrane domains of G-protein coupled receptors as a template for our 5-HT_7 receptor model, instead of the X-ray structure of bovine rhodopsin with a 2.6 Å resolution, published in 2000.[32] In our view, bovine rhodopsin, with its low degree of homology with the 5-HT_7 receptor (ca 24% for the sequences of the TM domains), is not the ultimate template for homology modeling of all GPCRs. Initial study of the X-ray structure of bovine rhodopsin revealed that the distance between the hypothesized ligand-binding amino acid residues Asp162 and Thr244 of TM3 and TM5, respectively, is far too big (>16 Å) for serotonin and other agonists to be spanned. Furthermore, Lopez-Rodriguez et al.[33] very recently argued for a different orientation of (the upper part of) TM3 of the 5-HT_{1A} receptor, according to molecular dynamics studies with a model based on the X-ray structure of rhodopsin. In fact, this different orientation resembles more the structure of the Baldwin template with respect to the relative distances of TM3, TM5, and TM6—especially near the binding site—than it resembles the X-ray structure of rhodopsin. Since the endogenous ligands for this family of receptors ranges from small ions to polypeptides,[34] it is very unlikely that this particular model of the 5-HT_7 receptor should fit the structure of an X-ray structure of a very specific type of GPCR, namely one with a covalently bound "agonist", without any modifications. We acknowledge the significance of the recently elucidated X-ray structure, but refuse to accept this as the "Holy Grail" in homology modeling of GPCRs. The template used in our study incorporates structural information derived from the analysis of ca. 500 sequences of GPCRs. According to the procedure used to build our model, the relative distance and orientation of the hypothesized ligand-binding amino acid residues mentioned above are more likely to be able to interact with serotonin and other agonists with comparable geometry.

More generally, in our view, a receptor model for a specific receptor subtype has to be adapted to a particular conformation of the neurotransmitter involved, otherwise there is no reason for this subtype to exist. This adaptation process can involve small rotations and translations of some helices in such a way that a perfect match is found for this particular conformation in the receptor. The specific conformation of the neurotransmitter can be deduced from the resemblance of this conformation with that of some agonists. Previously, we successfully followed this procedure in the investigation of compounds with mixed D_2 and 5-HT_{1A} receptor affinities.[35]

Although several groups[12,22] recently reported on the 5-HT_7 pharmacophore (models primarily based on antagonists), we are the first to investigate a pharmacophore model exclusively based on agonists. From the results obtained in this study, we conclude that deficiency of a hydrogen-bond-accepting moiety at the central aromatic ring system can be compensated by the presence of a flat aromatic ring system at a distance of 4.04−4.28 Å from, and almost perpendicular to, the central aromatic ring system. This moiety can occupy a hypothesized lipophilic pocket hosted by residues of TM5 and TM6. Furthermore, two CoMFA models were developed on the basis of a set of these 20 ligands with structural variance, showing high R^2 values [0.978 (A1), and 0.991 (A2)] and acceptable standard errors of

estimates (0.214, and 0.138, respectively). Successively, the colored molecular areas, as computed from the CoMFA studies, were projected onto the binding site of the additionally developed homology model of the 5-HT$_7$ receptor. The areas could successfully be interrelated with amino acid side chains forming lipophilic pockets, causing steric repulsions and attractive electrostatic interactions. Docking studies of a number of ligands into the binding site of our receptor model resulted in properly minimized receptor−ligand complexes with lower energies than the sum of energies of free receptor and ligand.

Experimental Section

Synthesis of Ligands, General Remarks. All ligands used in this study have been reported previously and were synthesized according to the methods described in Schemes 1−3, unless stated otherwise, and purified by means of chromatography on silica gel (Merck 60) and generally eluted with various mixtures of solvents. The purity of the target compounds was established using multiple techniques. IR spectra were recorded on an ATI-Mattson Genesis Series FT-IR spectrophotometer. NMR data were obtained using a Varian VXR-300 spectrometer (^{1}H NMR at 300 MHz, ^{13}C NMR at 75 MHz). Electron impact (EI$^+$) mass spectra were recorded on a Unicam Automass mass spectrometer in conjunction with a gas chromatograph. TLC analyses were carried out on aluminum plates (Merck) precoated with silica gel 60 F_{254} (0.2 mm). Visualization of spots was performed with UV light and a commonly used alkaline $KMnO_4$ spray solution. All materials were purchased from commercial suppliers. Only THF and ether were distilled prior to use, and all other chemicals and solvents were used without further purification.

Conformational Analysis. All molecular modeling calculations were performed on a Silicon Graphics O2 workstation running IRIX 6.3. Ligands were sketched with the correct stereochemistry, if present, in their protonated, positively charged state from standard fragments in MacroModel.[28] Structures were minimized with default options prior to full conformational analysis. Conformational analyses were performed using the Monte Carlo Multiple Minimum (MCMM) search protocol[36] with a minimum of 1500 steps via the SUMM option.[37] Minimizations were performed using the Truncated Newton Conjugate Gradient (TNCG) minimization method within the MM3* force field[38−40] with simulation of a distance-dependent water continuum[41] as implemented in MacroModel. Per step, 250 iterations were performed until the gradient reached the value of 0.01 kcal Å^{-1} mol^{-1}. All conformations within a range of 50 kJ/mol above the global minimum were considered to be relevant. In the case of nonchiral ligands, mirror images were preserved using the NANT option. Additional information needed for subsequent calculations with the pharmacophore-identifying software program APOLLO was obtained through incorporation of DEBG options 3 and 28. Torsion bonds of *n*-propyl chains were fixed in their anti-staggered conformation to reduce the number of low-energy conformations. Molecular dimensions and atomic distances were determined by manual selection of the appropriate atomic features in the Analyze mode.

Pharmacophore Identification. The VECADD module of APOLLO[29] was used to define extension vectors and centroids to all low-energy conformations of all ligands as calculated by MacroModel in the previousy described section. Extension vectors were allocated to the lone-pairs of the oxygen atoms of substituents (if present) of the six-membered aromatic ring present in all ligands, and the protonated, positively charged nitrogen atom also present in all ligands. A centroid was defined for the six-membered aromatic ring present in all indole-, aminotetraline-, ergoline-, and phenylpiperazine-based ligands (in the case of **14** and **15**, the six-membered ring is not substituted with a piperazine moiety). Alternatively, in case of **17**, extension vectors were defined for the lone pairs of the oxygen atoms of the diethyl amide moiety. The RMSFIT module of APOLLO subsequently identified the conformations of the ligands that exhibited the best overall least-squares fit with respect to the specified extension vectors and centroids. This calculation was performed in an energy-dependent manor, while all fitting points were considered equally important. In case multiple solutions were calculated, the matches were ranked with respect to conformational energies and root-mean-square deviations. The best fit was extracted from the RMSFIT output file using the MMDFIT module of APOLLO.

CoMFA Computations. Selected conformations of the ligands were imported into a Sybyl[30] database as pdb files as selected by the APOLLO molecular modeling and extracted from the RMSFIT output file using the MMDFIT module. Atom types were checked and adjusted if necessary, extension vectors and centroids were deleted, and atomic charges were calculated (Gasteiger−Hückel). On the basis of this database, a new MSS was opened, and pK_i values were entered manually. CoMFA parameters calculated with Sybyl standard parameters and with steric and dielectric cutoff values of 15 and 10 kcal/mol, respectively (distance dependent dielectric function) were inserted as a separate column. For both alignments, six partial least squares (PLS) calculations were performed: five cross-validated (four groups) and one non-cross-validated.

5-HT$_7$ Receptor Binding Assay. Binding assays on membranes from HEK cells expressing rat 5-HT$_7$ (r5-HT$_7$; receptor (obtained from Dr. David Sibley) receptors were performed according to standard procedures. Briefly, cell paste was homogenized in 50 mM Tris HCl buffer (pH 7.4) containing 2.0 mM $MgCl_2$ using a hand-held Polytron (setting 6 for 10 s) and spun in a centrifuge at 40 000*g* for 10 min. The pellet was resuspended in 50 mM Tris HCl buffer (pH 7.4) containing 0.5 mM EDTA, 10 mM $MgSO_4$, 2 mM $CaCl_2$, 10 μM pargyline, and 0.1% ascorbic acid. Incubations were initiated by the addition of membranes (20 μg protein per well) to 96-well plates containing test drugs and 0.3 nM [^{3}H]-5-CT (final volume of 250 μL). Nonspecific binding was determined by radioligand binding in the presence of a saturating concentration of 5-HT (10 μM). After a 2-h incubation period at room temperature, assay samples were rapidly filtered through Whatman GF/B filters and rinsed with ice-cold 50 mM Tris buffer (pH 7.4) using a Skatron harvester (Molecular Devices). Membrane bound [^{3}H]-5-CT levels were determined by liquid scintillation counting of the filters in BetaScint. The IC_{50} value (concentration at which 50% inhibition of specific binding occurs) was calculated by linear regression of the log concentration−response data. K_i values were calculated according to the Cheng−Prusoff equation, $K_i = IC_{50}/(1 + (L/K_d))$, where L is the concentration of the radioligand used in the experiment and the K_d value is the dissociation constant for the radioligand (determined previously by saturation analysis).

5-HT$_7$ Adenylate Cyclase Assay. Effects on adenylate cyclase activity were measured according to previously published methods.[42] HEK-293 cells expressing the rat 5-HT$_7$ were grown in Dulbecco's modified Eagle's media (DMEM) containing 10% fetal bovine serum, 400 μg of G418 (Geneticin), and 2 mM glutamine until flasks were confluent. Cells from confluent flasks were harvested by replacing the media with phosphate-buffered saline (PBS) containing 5 mM EDTA (pH 7.4). Cells were homogenized in 5 mM HEPES buffer containing 1 mM EGTA (pH 7.4) using a hand-held glass−Teflon homogenizer. The homogenate was centrifuged at 35 000*g* for 10 min. The cell pellet was resuspended in 100 mM HEPES buffer containing 1 mM EGTA (pH 7.4). Membranes (30−40 μg protein) were incubated at 37°C in a reaction medium containing 100 mM Hepes (pH 7.4), 5.0 mM $MgCl_2$, 0.5 mM ATP, 1.0 mM cAMP, 0.5 mM IBMX, 10 mM phosphocreatine, 0.31 mg/mL creatine phosphokinase, 100 μM GTP, 1 μCi α-[^{33}P]ATP per tube, and test drugs (final volume of 100 μL). Incubations were terminated after 15 min by adding 2% sodium dodecyl sulfate. After separation of [^{33}P]cAMP from [^{33}P]ATP as described by Salomon, [^{33}P]cAMP levels were determined by liquid scintillation counting, with the results expressed as picomoles per minute

per milligram of protein. EC_{50} and IC_{50} values were calculated by linear regression analysis of the concentration−response curves. Efficacy values were calculated as the maximal effect of an agonist in terms of the maximal effect produced by a known agonist such as 5-HT. Apparent K_i values for antagonists were calculated as follows: $K_i = IC_{50}/(1 + (C/EC_{50}))$, where C is the concentration of the agonist used in the experiment and EC_{50} is the EC_{50} for the agonist.

References

(1) Vanhoenacker, P.; Haegeman, G.; Leysen, J. E. 5-HT7 receptors: Current knowledge and future prospects. *Trends. Pharmacol. Sci.* **2000**, *21*, 70−77.

(2) Eglen, R. M.; Jasper, J. R.; Chang, D. J.; Martin, G. R. The 5-HT7 receptor: Orphan found. *Trends. Pharmacol. Sci* **1997**, *18*, 104−107.

(3) Terron, J. A. The 5-HT7 receptor: A target for novel therapeutic avenues? *Drugs* **1998**, *1*, 302−310.

(4) Bard, J. A.; Zgombick, J.; Adham, N.; Vaysse, P.; Branchek, T. A.; Weinshank, R. L. Cloning of a novel human serotonin receptor (5-HT7) positively linked to adenylate cyclase. *J. Biol Chem.* **1993**, *268*, 23422−23426.

(5) Ruat, M.; Traiffort, E.; Leurs, R.; Tardivel Lacombe, J.; Diaz, J.; Arrang, J.; Schwartz, J. C. Molecular cloning, characterization, and localization of a high-affinity serotonin receptor (5-HT7) activating cAMP formation. *Proc. Natl. Acad. Sci U.S.A.* **1993**, *90*, 8547−8551.

(6) Heidmann, D. E.; Metcalf, M. A.; Kohen, R.; Hamblin, M. W. Four 5-hydroxytryptamine7 (5-HT7) receptor isoforms in human and rat produced by alternative splicing: Species differences due to altered intron-exon organization. *J. Neurochem.* **1997**, *68*, 1372−1381.

(7) Jasper, J. R.; Kosaka, A.; To, Z. P.; Chang, D. J.; Eglen, R. M. Cloning, expression and pharmacology of a truncated splice variant of the human 5-HT7 receptor (h5-HT7b). *Br. J. Pharmacol.* **1997**, *122*, 126−132.

(8) Stam, N. J.; Roesink, C.; Dijcks, F.; Garritsen, A.; van Herpen, A.; Olijve, W. Human serotonin 5-HT7 receptor: Cloning and pharmacological characterisation of two receptor variants. *FEBS Lett.* **1997**, *413*, 489−494.

(9) Forbes, I. T.; Dabbs, S.; Duckworth, D. M.; Jennings, A. J.; King, F. D.; Lovell, P. J.; Brown, A. M.; Collin, L.; Hagan, J. J.; Middlemiss, D. N.; Riley, G. J.; Thomas, D. R.; Upton, N. (*R*)-3,*N*-dimethyl-*N*-[1-methyl-3-(4-methyl-piperidin-1-yl)propyl]benzenesulfonamide: The first selective 5-HT7 receptor antagonist. *J. Med. Chem.* **1998**, *41*, 655−657.

(10) Linnanen, T. Serotonergic Aporphine Derivatives, Thesis, Uppsala University, 2000.

(11) Kikuchi, C.; Nagaso, H.; Hiranuma, T.; Koyama, M. Tetrahydrobenzindoles: Selective antagonists of the 5-HT7 receptor. *J. Med. Chem.* **1999**, *42*, 533−535.

(12) Lopez-Rodriguez, M. L.; Porras, E.; Benhamu, B.; Ramos, J. A.; Morcillo, M. J.; Lavandera, J. L. First pharmacophoric hypothesis for 5-HT7 antagonism. *Bioorg. Med. Chem. Lett.* **2000**, *10*, 1097−1100.

(13) Lovenberg, T. W.; Baron, B. M.; de Lecea, L.; Miller, J. D.; Prosser, R. A.; Rea, M. A.; Foye, P. E.; Racke, M.; Slone, A. L.; Siegel, B. W. A novel adenylyl cyclase-activating serotonin receptor (5-HT7) implicated in the regulation of mammalian circadian rhythms. *Neuron* **1993**, *11*, 449−458.

(14) Jacobs, E. H.; Yamatodani, A.; Timmerman, H. Is histamine the final neurotransmitter in the entrainment of circadian rhythms in mammals? *Trends. Pharmacol. Sci.* **2000**, *21*, 293−298.

(15) Ying, S. W.; Rusak, B. 5-HT7 receptors mediate serotonergic effects on light-sensitive suprachiasmatic nucleus neurons. *Brain Res.* **1997**, *755*, 246−254.

(16) Mullins, U. L.; Gianutsos, G.; Eison, A. S. Effects of antidepressants on 5-HT7 receptor regulation in the rat hypothalamus. *Neuropsychopharmacology* **1999**, *21*, 352−367.

(17) Duncan, M. J.; Short, J.; Wheeler, D. L. Comparison of the effects of aging on 5-HT7 and 5-HT1A receptors in discrete regions of the circadian timing system in hamsters. *Brain Res.* **1999**, *829*, 39−45.

(18) Yau, J. L.; Noble, J.; Widdowson, J.; Seckl, J. R. Impact of adrenalectomy on 5-HT6 and 5-HT7 receptor gene expression in the rat hippocampus. *Mol. Brain Res.* **1997**, *45*, 182−186.

(19) Shimizu, M.; Nishida, A.; Zensho, H.; Yamawaki, S. Chronic antidepressant exposure enhances 5-hydroxytryptamine7 receptor-mediated cyclic adenosine monophosphate accumulation in rat frontocortical astrocytes. *J. Pharmacol. Exp. Ther.* **1996**, *279*, 1551−1558.

(20) Terron, J. A.; Falcon Neri, A. Pharmacological evidence for the 5-HT7 receptor mediating smooth muscle relaxation in canine cerebral arteries. *Br. J. Pharmacol.* **1999**, *127*, 609−616.

(21) De Vries, P.; De Visser, P. A.; Heiligers, J. P. C.; Villalon, C. M.; Saxena, P. R. Changes in systemic and regional haemodynamics during 5-HT7 receptor-mediated depressor responses in rats. *Naunyn S. Arch. Pharmacol.* **1999**, *359*, 331−338.

(22) Wilcox, R. E.; Ragan, J. E.; Pearlman, R. S.; Brusniak, M. Y.; Eglen, R. M.; Bonhaus, D. W.; Miller, J. D. High-affinity interactions of ligands at recombinant guinea pig 5HT7 receptors. *J. Comput. Aided Mol. Des.* **2001**, *15*, 883−909.

(23) Baldwin, J. M.; Schertler, G. F. X.; Unger, V. M. An alpha-carbon template for the transmembrane helices in the rhodopsin family of G-protein-coupled receptors. *J. Mol. Biol.* **1997**, *272*, 144−164.

(24) Parikh, V.; Welch, W. M.; Schmidt, A. W. Discovery of a series of (4,5-Dihydroimidazol-2-yl)-biphenylamine 5-HT(7) agonists. *Bioorg. Med. Chem. Lett.* **2003**, *13*, 269−271.

(25) Plassat, J. L.; Amlaiky, N.; Hen, R. Molecular cloning of a mammalian serotonin receptor that activates adenylate cyclase. *Mol. Pharmacol.* **1993**, *44*, 229−236.

(26) Sanin, A.; Brisander, M.; Rosqvist, S.; Mohell, N.; Malmberg, A.; Johansson, A. M., 5-Aryl substituted (*S*)-2-(dimethylamino)-tetralines. Novel serotonin 5-HT7 receptor ligands, poster at XVIIth Int. Symp. Medicinal Chemistry, Barcelona, 2002.

(27) Shen, Y.; Monsma, F. J., Jr.; Metcalf, M. A.; Jose, P. A.; Hamblin, M. W.; Sibley, D. R. Molecular cloning and expression of a 5-hydroxytryptamine7 serotonin receptor subtype. *J. Biol Chem.* **1993**, *268*, 18200−18204.

(28) MacroModel, Version 7.0.; Schrodinger Inc., 1999.

(29) Snyder, J. P.; Rao, S. N.; Koehler, K. F.; Vedani, A.; Pelliciari, R. APOLLO Pharmacophores and the pseudoreceptor concept, in *Trends in QSAR and Molecular Modeling 92*, Wermuth, C. G., Ed.; ESCOM: Leiden, 1993; pp 44−51.

(30) Sybyl Molecular Modeling Software, Version 6.8; Tripos, Inc., 2001.

(31) Javitch, J. A.; Ballesteros, J. A.; Weinstein, H.; Chen, J. A cluster of aromatic residues in the sixth membrane-spanning segment of the dopamine D2 receptor is accessible in the binding-site crevice. *Biochemistry* **1998**, *37*, 998−1006.

(32) Palczewski, K.; Kumasaka, T.; Hori, T.; Behnke, C. A.; Motoshima, H.; Fox, B. A.; Le, T., I.; Teller, D. C.; Okada, T.; Stenkamp, R. E.; Yamamoto, M.; Miyano, M. Crystal structure of rhodopsin: A G protein-coupled receptor [see comments]. *Science* **2000**, *289*, 739−745.

(33) Lopez-Rodriguez, M. L.; Vicente, B.; Deupi, X.; Barrondo, S.; Olivella, M.; Morcillo, M. J.; Behamu, B.; Ballesteros, J. A.; Salles, J.; Pardo, L. Design, synthesis and pharmacological evaluation of 5-hydroxytryptamine(1a) receptor ligands to explore the three-dimensional structure of the receptor. *Mol. Pharmacol.* **2002**, *62*, 15−21.

(34) Rim, J.; Oprian, D. D. Constitutive activation of opsin: Interaction of mutants with rhodopsin kinase and arrestin. *Biochemistry* **1995**, *34*, 11938−11945.

(35) Homan, E. J.; Wikstrom, H. V.; Grol, C. J. Molecular modeling of the dopamine D2 and serotonin 5-HT1A receptor binding modes of the enantiomers of 5-OMe-BPAT. *Bioorg. Med. Chem.* **1999**, *7*, 1805−1820.

(36) Chang, G.; Guida, W. C.; Still, W. C. An internal-coordinate Monte Carlo method for searching conformational space. *J. Am. Chem. Soc.* **1989**, *111*, 4379−4386.

(37) Goodman, J.; Still, W. C. An unbounded systematic search of conformational space. *J. Comput.Chem.* **1991**, *12*, 1110−1117.

(38) Allinger, N. L.; Yuh, Y. H.; Lii, J.-H. Molecular mechanics. The MM3 force field for hydrocarbons. 1. *J. Am. Chem. Soc.* **1989**, *111*, 8551−8566.

(39) Lii, J.-H.; Allinger, N. L. Molecular mechanics. The MM3 force field for hydrocarbons. 2. Vibrational frequencies and thermodynamics. *J. Am. Chem. Soc.* **1989**, *111*, 8566−8575.

(40) Lii, J.-H.; Allinger, N. L. Molecular mechanics. The MM3 force field for hydrocarbons. 3. The van der Waals' potentials and crystal data for aliphatic and aromatic hydrocarbons. *J. Am. Chem. Soc.* **1989**, *111*, 8576−8582.

(41) Still, W. K.; Tempczyk, A.; Hawley, R. C.; Hendrickson, T. Semianalytical treatment of solvation for molecular mechanics and dynamics. *J. Am. Chem. Soc.* **1990**, *112*, 6127−6129.

(42) Salomon, Y. Adenylate Cyclase Assay. *Adv. Cyclic Nucleotide Res.* **1979**, *10*, 35−55.

JM030826M